Inorg. Chem. **2007**, *46*, 6022–6028

Different Cation Arrangements in Au–In Networks. Syntheses and Structures of Six Intermetallic Compounds in Alkali-Metal–Au–In Systems

Bin Li and John D. Corbett*

Ames Laboratory−DOE and Department of Chemistry, Iowa State University, Ames, Iowa 50011

Received March 17, 2007

Six robust intermetallic compounds with cations in three different tunnel-like structures have been synthesized in alkali-metal–Au–In systems via high-temperature solid-state methods and characterized by X-ray diffraction: AAu_4In_6 [A = K (**I**), Rb (**II**), $P\bar{6}m2$, $Z = 1$], $K_{1.76(6)}Au_6In_4$ (**III**, $I4/mcm$, $Z = 4$), and $A_xAu_2In_2$ [$x \approx 0.7$, A = K (**IV**), Rb (**V**), Cs (**VI**), $P4_2/nmc$, $Z = 8$]. The first type is constructed from a single cage unit: an alkali-metal-centered 21-vertex polyhedron $A@Au_9In_{12}$ with 6-9-6 arrangement of planar rings. The others contain uniaxial arrays of tunnels built of differently puckered eight- and four-member Au/In rings. The largely different cation distributions depend on the tunnel constitutions and cation sizes. Tight-binding electronic structure calculations by linear muffin-tin-orbital (LMTO) methods were performed for **I** and idealized **III** in order to help understand their chemical bonding. These also reveal large differences in relativistic effects for Au d orbitals, as well as for different Au sites in each structure.

Introduction

Explorations of binary alkali-metal−triel (A−Tr) systems have led to the discovery of many new compounds with novel structural and bonding features.[1] Inclusion of a third heteroelement, either another alkali or alkaline-earth metal or a late transition metal, has proven to be a very effective route to diverse new cluster structures, evidently because different mixed atom sizes, valence electron counts, and/or bond strengths afford a great deal of flexibility. Owing to the pronounced differences in electronegativities between the triel metals and the alkali or alkaline-earth metals, the triels usually form clusters that are interbonded or linked into three-dimensional network structures in which the alkali or alkaline-earth metals are encapsulated. The differences in electronegativities between the added third element and the other two elements are quite important in the formation of the structures. A late transition metal that has an electronegativity greater than that of the triel usually participates in the polyanionic part with the triel, such as in Na_3MIn_2 (M = Au, Ag),[2] $Na_{13}(Cd_{\sim 0.70}Tl_{\sim 0.30})_{27}$,[3] and $K_{34}Au_{8.81(6)}In_{96.19(6)}$.[4] The last compound, the first ternary compound in K−Au−In system, contains a mixed Au/In anionic network, resembling much more the distributions of Li, Mg, and Zn in $K_{34}In_{92.30(7)}Li_{12.70}$,[5] $K_{34}In_{91.05(9)}Mg_{13.95}$, and $K_{34}Zn_{13.05(7)}In_{89.95(1)}$,[4] respectively.

Our recent research in alkali-metal−Au−In systems revealed a new Au−In framework $K_xRb_{1-x}Au_4In_2$ ($x = 0-1$) with a uniaxial tunnel structure, analogous to those of some microporous zeolites.[6] The phase is also quite inert to air, water, and concentrated HCl(aq) at room temperature. The interesting tunnel character and inertness have motivated us to explore for other structures in such systems. On the other hand, quite different Au−In frameworks have been found in the Na−Au−In system, e.g., in $NaAuIn_2$,[7] $Na_2Au_6In_5$,[8] $Na_8Au_{11}In_6$,[9] and Na_3AuIn_2.[2] Surprisingly, none of them has an Au−In framework similar to those considered here, perhaps because of the smaller cation size and greater sodium participation in the bonding.[2] Here we report the syntheses

* To whom correspondence should be addressed. E-mail: jcorbett@iastate.edu.

(1) (a) Corbett, J. D. In *Chemistry, Structure and Bonding of Zintl Phases and Ions*; Kauzlarich S., Ed.; VCH Publishers: New York, 1996; Chapter 3. (b) Corbett, J. D. *Angew. Chem., Int. Ed.* **2000**, *39*, 670. (c) Belin, C. H. E.; Charbonnel, M. *Prog. Solid State Chem.* **1993**, *22*, 59.

(2) Li, B.; Corbett, J. D. *Inorg. Chem.* **2005**, *44*, 6515.
(3) Li, B.; Corbett, J. D. *Inorg. Chem.* **2004**, *43*, 3582.
(4) Li, B.; Corbett, J. D. *Inorg. Chem.* **2006**, *45*, 8958.
(5) Li, B.; Corbett, J. D. *J. Am. Chem. Soc.* **2005**, *127*, 926.
(6) Li, B.; Corbett, J. D. *J. Am. Chem. Soc.* **2006**, *128*, 12392.
(7) Zachwieja, U. *Z. Anorg. Allg. Chem.* **1995**, *621*, 1677.
(8) Zachwieja, U. *J. Alloys Comp.* **1996**, *235*, 7.
(9) Zachwieja, U. *Z. Anorg. Allg. Chem.* **1996**, *622*, 1581.

10.1021/ic700519c CCC: $37.00
Published on Web 06/20/2007

and structural characterizations of six additional intermetallic compounds in three different structures: AAu_4In_6 [A = K (**I**), Rb (**II**)], $K_{1.76(6)}Au_6In_4$ (**III**), and $A_xAu_2In_2$ [A = K (**IV**), Rb (**V**), and Cs (**VI**), $x \approx 0.7$]. The first two are isotypic with $LiCo_6P_4$,[10] and the other two represent new structural types.

Experimental Section

Syntheses. All materials were handled in N_2-filled gloveboxes with moisture levels below 1 ppm (vol). All compounds were synthesized via high-temperature reactions of the elements (99.95% potassium, 99.75% rubidium, 99.98% cesium, 99.99% indium, all from Alfa-Aesar, and 99.995% gold from the Ames Laboratory). The weighed elements were enclosed in tantalum tubes that were welded shut and in turn sealed into evacuated fused silica jackets as described previously.[11]

Single crystals of **I**, **III**, and **IV** were first obtained from reactions with loaded compositions of KAu_4In_4, KAu_3In_2, and KAu_2In_2, respectively, with an expectation of gaining tunnel structures similar to that of KAu_4In_2[6] The structures were refined in different space groups: $P\bar{6}m2$ (No.187, $Z = 1$) for **I**, $I4/mcm$ (No.140, $Z = 4$) for **III**, and $P4_2/nmc$ (No.137, $Z = 8$) for **IV**. All contain Au−In networks filled by K, the last two with fractional K occupancies. Once the stoichiometries had been established by crystallography, a single-phase sample (>95%) of each was synthesized as below from the appropriate refined compositions (as judged from comparisons of their Guinier powder patterns with those calculated from the refined structures). (K−In interference precluded EDAX analyses.) As expected, three other compounds with different cations, **II**, isostructural with **I**, and **V** and **VI**, both isostructural with **IV**, were similarly synthesized in pure phases and structurally characterized. No phase width in any of the compounds with a fractional atom site occupation, **III**−**VI**, was indicated by shifts of cell parameters for a product from reactions loaded with different alkali-metal proportions.

Both **I** and **II** were obtained from samples heated at 600 °C for 12 h, cooled at 10 °C/h to 450 °C, held there for 160 h to grow crystals, followed by cooling to room temperature at 5 °C/h. The same reaction profile was used for **III** except for quenching from 600 °C to room temperature before annealing at 350 °C. The quench process proved necessary to get a single phase. Pure **IV**, **V**, and **VI** were obtained by either a slow cool or quench process as above followed with annealing at 350 °C for 160 h. All compounds are brittle and silvery color, except for **III**, which has a light copper color. They all are inert to air at room temperature, moreover **I**, **II**, and **III** also appear to be inert to water at room temperature for >24 h inasmuch as their powder patterns showed no changes in the line intensities, breadths, or positions. Attempts to synthesize Na analogues all failed.

X-ray Studies. Powder diffraction data were collected with the aid of a Huber 670 Guinier powder camera equipped with an area detector and Cu Kα radiation ($\lambda = 1.540598$ Å). Powdered samples were homogeneously dispersed between two layers of Mylar with the aid of a little vacuum grease. Single crystals were selected from the products in a glovebox and, as an early precaution, sealed into capillaries. Single-crystal diffraction data for **I**, **II**, and **III** were collected at 293 K with Mo Kα radiation on a Bruker SMART APEX CCD diffractometer in the form of three sets of 606 frames with 0.3° scans in ω and exposures of 10 s per frame. The 2θ range extended from ~3° to ~57°. The reflection intensities were integrated with the SAINT subprogram in the SMART software package,[12] and the data were corrected for Lorentz and polarization effects. Diffraction data for **IV**, **V**, and **VI** were collected at 293 K and, for **IV,** again at 120K with the aid of a STOE IPDS II single-crystal X-ray diffractometer with Mo Kα radiation. The data collections, integrations, and corrections were carried out with the aid of the STOE software.[13] Numerical absorption corrections with the program X-shape[14] in STOE software were necessary to get reasonable refinements for all the compounds, except for **II**, which could also be refined well after the SADABS absorption correction.[15] For example, refinement without the numerical absorption correction gave $U_{11}/U_{33} > 25$ for K in **I** instead of 1.6 reported. The large single-crystal sizes, up to 0.31 mm maximum (Supporting Information, cif), and large proportions of gold were probably responsible for the requirement of numerical absorption corrections.

All structural solutions were obtained by direct methods and refined by full-matrix least-squares refinement on F_o^2 using the Bruker SHELXTL 6.1 software package.[16] The data sets of both **I** and **II** contained no systematic absences, and their intensity statistics gave clear indications of non-centrosymmetric space groups (for example, $| E^2 - 1 | = 0.765$ for K). The assignments of the extinction-free space group $P\bar{6}m2$ (No. 187) to both were also supported by the subsequent successful refinements. Direct methods provided four peaks for **I**, of which two were assigned to Au and two to In atoms according to peak heights and separations. A few least-squares cycles followed by a difference Fourier map revealed one less strongly diffracting atom with distances around it appropriate for K, and it was so assigned. The refined occupancy for each atom site was close to unity, ~1.00(1). The refinement, finally with anisotropic displacement parameters and a secondary extinction correction, converged at R1 = 0.026 ($I > 2\sigma(I)$) with the largest different peak of 1.8 e/ Å.[3] The structure of **II** was solved and refined on the basis of the model for **I**.

A data set from **III** showed a body-centered tetragonal lattice with *c* glide along the *a* axis, and intensity statistics indicated a centrosymmetric space group. So the structure was solved in the only possible space group $I4/mcm$, which is same as that of KAu_4In_2.[6] These two structures also have almost the same *a* and *b* axial lengths, but different *c* values. For **IV**, the only possible space group was $P4_2/nmc$ according to the systematic absences and intensity statistics. For both **III** and **IV**, direct methods provided all positions for Au, In, and K. However, a few least-squares cycles followed by a difference Fourier map revealed that K alone was too electron-rich in each K site in both structures, as indicated by their abnormally large isotropic displacements. At this point R1 ($I > 2\sigma(I)$) and the largest difference peak were 0.08 and 11.1 e/ Å^3 for **III** and 0.06 and 6.6 e/ Å^3 for **IV**, respectively. Variable-occupancy refinements for all K sites gave more reasonable isotropic displacement parameters, as well as small reductions in both R1 and the highest residual peaks. The final refinements with anisotropic displacement parameters converged at R1 ($I > 2\sigma(I)$) = 0.038 and 0.049 with the largest residual peaks of 3.0 and 3.7e/ Å^3 for **III** and **IV**, respectively. The structures of **V** and **VI** were similarly solved on the basis of model **IV**.

Compared with the fully occupied and well-ordered cation sites in both **I** and **II**, the cations in the other four compounds show partial occupancies and nearly continuous electron densities along

(10) Buschmann, R.; Schuster, H. U. *Z. Naturforsch.* **1991**, *46b*, 699.
(11) Dong, Z.-C.; Corbett, J. D. *J. Am. Chem. Soc.* **1993**, *115*, 11299.
(12) *SMART*; Bruker AXS, Inc.; Madison, WI, 1996.
(13) *IPDS II*; Stoe and Cie GmbH: Darmstadt, Germany, 2002.
(14) *XSHAPE 2.03*; Stoe and Cie GmbH: Darmstadt, Germany, 2003.
(15) Blessing, R. H. *Acta. Crystallogr.* **1995**, *A51*, 33.
(16) *SHELXTL*; Bruker AXS, Inc.: Madison, WI, 2000.

Table 1. Crystal and Refinement Data for Compounds **I**−**VI**

compounds	KAu_4In_6 (**I**)	$RbAu_4In_6$ (**II**)	$K_{1.76(6)}Au_6In_4$ (**III**)	$K_{0.73(5)}Au_2In_2$ (**IV**)	$Rb_{0.66(2)}Au_2In_2$ (**V**)	$Cs_{0.66(1)}Au_2In_2$ (**VI**)
fw	1515.89	1562.26	1710.97	652.51	680.20	710.63
space group, Z	$P\bar{6}m2$, 1	$P\bar{6}m2$, 1	$I4/mcm$, 4	$P4_2/nmc$, 8	$P4_2/nmc$, 8	$P4_2/nmc$, 8
data collection	SMART APEX CCD	SMART APEX CCD	SMART APEX CCD	STOE IPDS II	STOE IPDS II	STOE IPDS II
unit cell (Å), a	8.058(1)	8.079(1)	8.665(1)	13.111(2)	13.305(1)	13.410(1)
c	4.4411(9)	4.4857(9)	14.190(3)	5.440(1)	5.460(1)	5.367(1)
V (Å^3)	249.74(7)	253.54(7)	1065.4(3)	935.1(3)	966.5(3)	965.2(3)
d_{calcd} (g/cm^3)	10.08	10.23	10.67	9.27	9.35	9.78
μ, mm^{-1} (Mo Kα)	72.40	75.68	91.38	72.75	76.38	74.62
data/restraints/params	265/0/19	269/0/19	371/0/23	689/0/31	550/0/31	604/0/31
GOF on F^2	1.16	1.13	0.83	0.99	0.86	1.21
R1/wR2 [$I > 2\sigma(I)$]	0.026/0.058	0.038/ 0.105	0.038/ 0.096	0.049/ 0.090	0.048/0.093	0.036/0.079
R1/wR2 (all data)	0.028/ 0.0586	0.039/ 0.104	0.048/ 0.099	0.094/ 0.105	0.140/0.112	0.069/0.083
diff peak and hole (e.Å^{-3})	1.75 and −1.74	2.10 and −2.99	2.96 and −2.91	3.69 and −2.34	3.26 and −2.13	1.81/-1.97

Table 2. Atomic Coordinates and Anisotropic Displacement Parameters (Å$^2 \times 10^3$)[a] for **I**, **III**, and **IV**

atom	site	x	y	z	U(eq)	U_{11}	U_{22}	U_{33}	occ.≠1
				KAu_4In_6 (**I**)					
Au1	1*c*	1/3	2/3	0	23(1)	23(1)	23(1)	22(1)	
Au2	3*k*	0.7944(1)	$-x$	1/2	24(1)	23(1)	23(1)	25(1)	
In1	3*k*	0.1954(2)	$-x$	1/2	23(1)	22(1)	22(1)	25(1)	
In2	3*j*	0.5342(2)	$-x$	0	24(1)	26(1)	26(1)	21(1)	
K	1*a*	0	0	0	27(2)	31(4)	31(4)	19(5)	
				$K_{1.76(6)}Au_6In_4$ (**III**)					
Au1	8*h*	0.1588(1)	$x + 1/2$	0	27(1)	31(1)	31(1)	18(1)	
Au2	16*l*	0.1549(1)	$x + 1/2$	0.1949(1)	26(1)	30(1)	30(1)	18(1)	
In	16*l*	0.6386(1)	$x + 1/2$	0.1080(1)	22(1)	23(1)	23(1)	21(1)	
K1	4*a*	0	0	1/4	112(14)	21(6)	21(6)	300(40)	0.87(6)
K2	4*c*	0	0	0	200(20)	13(6)	13(6)	570(70)	0.89(6)
				$K_{0.73(5)}Au_2In_2$ (**IV**)					
Au1	8*g*	1/4	0.0750(1)	0.3747(2)	26(1)	32(1)	18(1)	28(1)	
Au2	8*g*	1/4	0.5763(1)	0.0237(2)	27(1)	32(1)	20(1)	29(1)	
In1	8*g*	1/4	0.1263(2)	0.8670(4)	24(1)	24(1)	22(1)	27(1)	
In2	8*g*	1/4	0.6263(2)	0.5276(4)	24(1)	22(1)	19(1)	29(1)	
K	8*f*	0.500(1)	$-x$	1/4	350(50)	37(6)	37(6)	970(160)	0.73(5)

[a] The remaining U_{ij} data are in the cif data.

the tunnel centers, which are better displayed in their Fourier maps (Figure S1). Attempts to find better solutions in lower symmetry space groups still yielded unusual anisotropic parameters for the cations, as well as some short cation−cation distances between fractional atoms. The refinement of data for **IV** collected at 120 K also shows essentially the same K displacements, which indicated that the extremes are more related to intrinsic disorder rather than actual thermal displacements, as expected. The presence of any superstructure or incommensurate structure, which might generate the unusual displacements and occupancy features, was not supported by the observation of additional or irregular Bragg reflections on the STOE diffractometer.

Some crystallographic and refinement parameters for all six compounds are given in Table 1. Table 2 gives the corresponding atomic positional and anisotropic displacement parameters for the three K compounds. The atomic positions in all compounds, as well as their anisotropic displacement parameters, are given in Table S1. Table 3 contains important interatomic distances for the three K compounds. More detailed crystallographic and refinement data for all six compounds are available in the Supporting Information (cif).

Electronic Structure Calculations. In order to better understand the chemical bonding and the relativistic (scalar) effects of Au, tight-binding electronic structure calculations were performed for **I** and **III** by the linear muffin-tin-orbital (LMTO) method in the atomic sphere approximation (ASA).[17] The calculations for **III** were carried out on the hypothetical composition $K_2Au_6In_4$ with full K occupancies. The radii of the Wigner−Seitz (WS) spheres were assigned automatically so that the overlapping potentials would be the best possible approximations to the full potentials,[18] and no interstitial sphere was necessary with the 18% overlap restriction. The WS radii determined by this procedure were about 1.56 Å for In, 1.50 Å for Au in both cases, 2.19 Å for K in **I**, and 2.02 and 1.94 Å for K1 and K2 in **III**, respectively. The smaller WS radii for the cations in **III** are related to their partial occupancies.

Table 3. Selected Bond Lengths [Å] for **I**, **III**, and **IV**

KAu_4In_6 (**I**)		$K_{1.76}Au_6In_4$ (**III**)		$K_{0.73}Au_2In_2$ (**IV**)	
Au1−In2	2.804(3)	Au1−Au2	2.767(1)	Au1−In1	2.761(2)
Au1−In1	2.939(2)	Au1−In	2.917(2)	Au1−Au2	2.754(1)
Au2−In1	2.801(1)	Au1−In	3.003(2)	Au1−In2	2.768(2)
Au2−In2	2.869(1)	Au2−In	2.804(2)	Au1−In1	2.809(2)
Au2−Au2	3.088(2)	Au2−Au2	2.807(2)	Au1−In1	2.843(2)
In1−In2	3.332(2)	Au2−In	2.816(2)	Au2−In2	2.777(3)
In1−In1	3.335(5)	Au2−In	2.830(2)	Au2−In1	2.790(2)
In2−In2	3.201(4)	Au2−Au2	3.106(2)	Au2−In2	2.819(3)
K−In1	3.517(2)	In−In	3.064(3)	In1−In1	3.243(4)
K−Au2	3.628(1)	K1−Au2	3.3697(6)	In2−In2	3.333(4)
K−In2	4.057(2)	K1−In	3.913(1)	K−Au1	3.492(12)
K−K	4.441(1)	K2−In	3.687(1)	K−Au2	3.65(2)
		K2−Au1	3.2609(7)	K−Au2	3.73(2)
		K1−K2	3.5474(7)	K−In1	3.725(8)
				K−In2	3.86(2)
				K−K	2.7201(6)

(17) van Schilfgarde, M.; Paxton, T. A.; Jepsen, O.; Andersen, O. K.; Krier, G. *Program TB-LMTO*; Max-Plank-Institut für Festkörperforschung: Stuttgart, Germany, 1994.

(18) Tank, R.; Jepsen, O.; Burckhardt, A.; Andersen, O. K. *Z. Phys. B* **1995**, *97*, 35.

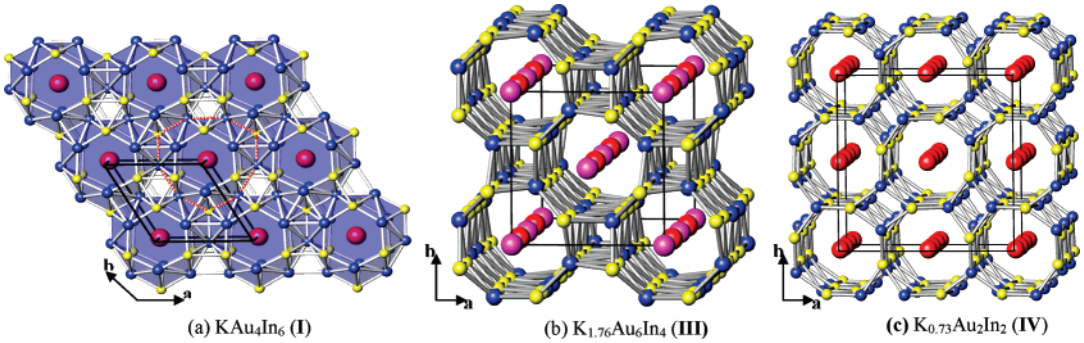

Figure 1. General ~[001] sections of (a) KAu_4In_6 (**I**) ($P\bar{6}m2$), (b) $K_{1.76}Au_6In_4$ (**III**) ($I4/mcm$), and (c) $K_{0.73}Au_2In_2$ (**IV**) ($P4_2/nmc$). The In, Au, and K atoms are blue, yellow, and red/fuchsia, respectively. The outer nonagon in **I** is marked with a red/white dotted line.

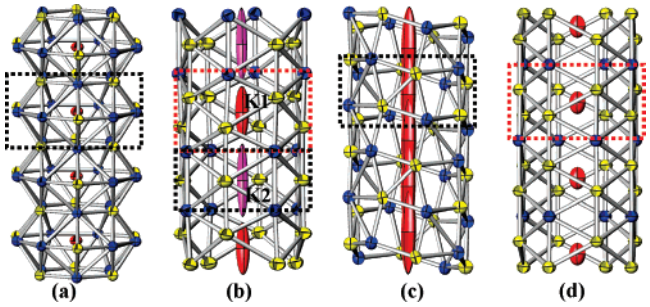

Figure 2. Different tunnels in (a) KAu_4In_6 (**I**), (b) $K_{1.76}Au_6In_4$ (**III**), (c) $K_{0.73}Au_2In_2$ (**IV**), and (d) KAu_4In_2 (ref 6) with the tunnel repeat units outlined. The In, Au, and K atoms are blue, yellow, and red/fuchsia, respectively (80% displacement ellipsoids).

However, the influence of these is negligible since the contributions from both K are very small, and the results depend mainly on the anionic networks.

Results and Discussion

Crystal Structures. KAu_4In_6 (I) and $RbAu_4In_6$ (II). The overview of their structure, Figure 1a, illustrates the three-dimensional Au−In network projected along the *c* axis. The structure is constructed from a single basic building unit: a 21-vertex polyhedron, $K@Au_9In_{12}$, as outlined in Figure 2a. This polyhedron can be described as an almost perfect hexagonal prism augmented by nine outer atoms in an In_6-Au_3 nonagon about the waist that is coplanar with K, i.e., a 6-9-6 arrangement of parallel planar rings. The bonds defining the six-member rings have the same lengths, 2.801 Å, but the angles In−Au−In and Au−In−Au are 115° and 125°, respectively. In the *ab* plane each polyhedron shares all six Au−In edges in the outer nine-member ring (red/white dotted in Figure 1a) with six other like polyhedra. In addition, the atoms in each six-member ring are connected to six other like rings via Au−Au (3.09 Å) and In−In (3.34 Å) separations, both of which are relatively long compared with their normal bond distances,[4,6] but still weakly bonding (below). The 21-vertex polyhedra stack along the *c* axis by sharing the hexagonal faces to form infinite tunnels, Figure 2a. This structure is isotypic with $LiCo_6P_4$,[10] which can likewise be described in terms of a single basic building unit: a 21-vertex polyhedron centered by lithium, $Li@P_9$-Co_{12}, comparable to the $A@Au_9In_{12}$. However, the former displays a very long P1−P1 distance between two polyhedra, 3.01 Å, too large for a significant bond.

$K_{1.76}Au_6In_4$ (III) and $K_{0.73}Au_2In_2$ (IV). Parts b and c of Figure 1 give overviews of the structures of body-centered tetragonal **III** and primitive tetragonal **IV**, respectively, via projections along their *c* axes. Both Au−In frameworks contain differently puckered eight- and four-member rings stacked along *c* to form tunnels. Each network atom is common to one four-member and two eight-member tunnels. The latter encapsulate the potassium cations as seen in Figure 2b and c, as well as the Rb (**V**) and Cs (**VI**) cations in salts that are isostructural with **IV**. Better representations of the cation environments with their nearest neighbors for all four compounds **III**−**VI** appear as Fourier maps in Figure S2. The two tunnel systems are defined by different repeating units as marked in Figure 2. The eight-member tunnels in **III**, Figure 2b, consist of two kinds of crownlike units condensed along *c*: $[In_{4/2}Au_4Au_4In_{4/2}]$ centered by K1 (dotted red lines) and $[In_{4/2}Au_4In_{4/2}]$ centered by K2 (dotted black lines). The former is the sole repeating unit in KAu_4In_2,[6] Figure 2d, which has the same space group, as well as about the same *a* and *b* axes as **III**, but a shorter *c* axis. In **IV** (**V**, **VI**) (Figure 2c), each K (Rb, Cs) is nominally at the center of a $[Au_{4/2}In_{4/2}Au_{4/2}In_{4/2}]$ unit in which the eight members of each ring are more nearly planar than in other compounds. In both structure types, the large tunnels are interconnected by In−Au exo bonds which define the four-member tunnels. In great contrast, **I**, Figure 2a, has a single and totally different basic building unit: a more condensed K-centered 21-vertex polyhedron, $K@Au_9In_{12}$, that shares six edges of the central nine-member rings, as well as the hexagonal faces with other like units.

Cation Dispositions. Both K and Rb sites in **I** and **II** are fully occupied, are well-ordered, and show normal distances to neighboring cations, whereas cations in the other two structures are fractional, marginally localized and, formally, less well separated. Distances refined between cations in **IV**, $K_{0.73}Au_2In_2$, as well as in the Rb and Cs analogues, are rather short, ~2.7 Å. However, the accuracies or meanings of the refined occupancies are somewhat doubtful, in parallel with an improbable credibility of the corresponding displacement ellipsoids refined. The former is most uncertain, 76(5)% for K, and it was obtained simultaneously with an extreme centric displacement ellipsoid along the tunnel with an aspect ratio of 26:1. The more meaningful Fourier map of this tunnel region (Supporting Information) suggests additional distor-

tions in the form of pronounced "warts" on the side walls. The analogous maps for the Rb and Cs isotypes suggest even more disorder, the latter showing six small but distinct maxima in the electron density "streak". The "best fit" ellipsoid now has an aspect ratio of ~77:1, so the 66(1)% occupancy may have limited analytical meaning. Under these circumstances, the refined intercationic distances appear to have similarly uncertain meanings. All other bond distances in the six compounds, including those between these fractional cations and the atoms in the tunnel walls, are comparable to those in other alkali-metal−Au−In compounds.[4, 6]

The cations in all structures are differently trapped in the infinite tunnels depending on what can be estimated as the relative "free" diameters of the tunnels. The smallest apertures along these are all defined by indium here. Considering the shorter unconstrained K−In distances in most intermetallic compounds,[1b,19] ~3.65 Å, and a 'hard' K^+ crystal radius, 1.52 Å (CN = 6),[20] we can assign indium a relative van der Waals radius of about 2.13 Å for the rigid hard-sphere model. From this, the smallest free apertures along the tunnels in AAu_4In_6 (**I** and **II**) at the planar six-member ring leave "free" radii of only ~0.60 and 0.62 Å for K and Rb, respectively. These values, much less than the six-coordinate crystal radii of K^+ and Rb^+ (1.66 Å),[20] are probably of limited value because the reference radii used come from situations with relatively weak interionic interactions together with standard assumptions about such relative radii.[21] The trends are still reasonable; the K atoms sit in rather open undifferentiated tunnels in both **III** and **VI**, Figure 2, even though the free radii so defined, 1.22 and 1.37 Å, respectively, are still smaller. The situation in KAu_4In_2[6] (1.19 Å) is very similar to that in **III** and in any case the absence of cation vacancies precludes any concerted hopping motions. All of the crystallographic results doubtlessly represent more static, long-term disorders rather than time-dependent processes. A hard-sphere model would not be suitable for a dynamic process either.

Compared with these encapsulated cations, remarkably specific but different alkali-metal dispositions about each anionic cluster have been found in alkali-metal-rich triel systems before.[1b] The cations often (1) cap cluster faces, (2) bridge edges, and (3) are positioned exo (outward) at vertices in order of increasing distance from the anion. Moreover, more than a dozen structures have been recently found to have regular cation arrangements with pentagonal dodecahedra A_{20} (A = alkali-metal) and hexakaidecahedra A_{28} capping the different sized triel polyhedra.[4,6,22] However, large decreases in alkali-metal proportions change cation dispositions relative to anionic networks, as in $K_3Mg_{20}In_{14}$,[23] KAu_4In_2,[6] and in the structures reported here in which the cations are trapped within anionic polyhedra or tunnels. Trapped cations are more frequent in alkaline earth metal−triel systems, and the overall drive for this can be interpreted as the need to give each cation as many close neighbors as possible in the more anionic network.[24] Both $AeMg_5In_3$[25] and AAu_4In_6 (**I** and **II**) contain 21-vertex polyhedra with similar 6-9-6 arrangements, i.e., $Ae@In_9Mg_{12}$ vs $A@Au_9In_{12}$, but the former is more distorted because of condensation. A similar arrangement with a K-centered 22-vertex polyhedron, $K@Mg_{12}In_{10}$, in a 1-6-8-6-1 arrangement occurs in $K_3Mg_{20}In_{14}$.[23] The need to give each cation as many close neighbors as possible is also shown in some contrary changes in atom distances in **I** and **II**. From K to Rb compounds, both the A−In and A−Au distances only increase about 0.035 Å, whereas all interbridging distances contrarily decrease: Au2−Au2 from 3.088(2) to 3.061(2) Å and In1−In1 from 3.335(5) to 3.312(3) Å. All of these changes favor the maintenance of a compact polyhedron around each cation.

Cation Displacements. The different cation displacements in the tunnels are another interesting feature in such structures. Elongation of the atom distributions is quite typical for tunnel-like structures with large cations, such as $K_{0.4}Cd_2$,[26] $NaGaSn_2$,[27] and all hollandite-type compounds.[28] The cations in **III**−**VI**, all of which have larger free radii in the tunnels, show large displacements along the tunnel directions, Figure 2b and c. The relative displacements of K1 and K2 in **III** are u_c/u_a = 0.55/0.14 and 0.75/0.11 Å, respectively (u_c and u_a are the square roots of U_{33} and U_{11} in tetragonal systems, respectively[29]). The difference between K1 and K2 might originate from their totally different coordinations (Figure S2). The former is surrounded by 16 Au/In atoms, and the latter by eight when K−Au/In separations less than 4 Å are considered, which gives K2 a corresponding larger elongation along the tunnel direction. The large cation displacements are also believed to be related to the cation sizes and the free radii defined by the tunnel atom arrangement. For example, the K in KAu_4In_2 has very similar coordinate environment as the K1 in **III** (red outlined units in Figure 2b and d), but the former shows normal atomic displacement, u_c/u_a =0.25/0.18,[6] probably because of its full occupancy and smaller free tunnel radius. In the three isostructural compounds **IV**, **V**, and **VI**, the cation displacements increase as the cation sizes increase, u_c/u_a = 0.98/0.19 Å for K, 1.03/0.18 Å for Rb, and 1.21/0.14 Å for Cs, although these changes may also include some compositional variations. Cation displacements along tunnel direction in series $K_xRb_{1-x}Au_4In_2$ ($x = 0-1$) also increase with an increased Rb proportion.[6] In contrast, both K and Rb in **I** and **II**, which are well trapped in 21-vertex polyhedron, show quite normal atomic displacements, a little larger in

(19) (a) Cordier, G.; Mueller, V. *Z. Kristallogr.* **1993**, *205*, 353. (b) Li, B.; Corbett, J. D. *Inorg. Chem.* **2002**, *41*, 3944. (c) Li, B.; Corbett, J. D. *Inorg. Chem.* **2003**, *42*, 8768.
(20) Shannon, R. D. *Acta. Crystallogr.* 1**976**, *A32*, 751.
(21) Shannon, R. D.; Prewitt, C. T. *Acta. Crystallogr.* 1**969**, *B25*, 925.
(22) Li, B.; Corbett, J. D. *Inorg. Chem.* **2003**, *42*, 8768.
(23) Li, B.; Corbett, J. D. *Inorg. Chem.* **2006**, *45*, 3861.
(24) Liu, S.; Corbett, J. D. *Inorg. Chem.* **2004**, *43*, 2471; Dai, J.-C.; Corbett, J. D. *Inorg. Chem.* **2007**, in press.
(25) Li, B.; Corbett, J. D. *Inorg. Chem.* **2007**, *46*, 2237.
(26) Todorov, E.; Sevov, S. C. *Inorg. Chem.* **1998**, *37*, 6341.
(27) Vaughey, J. T.; Corbett, J. D. *J. Am. Chem Soc.* **1996**, *118*, 12098.
(28) (a) Wu, X. J.; Fujiki, Y.; Ishigame, M.; Horiuchi, S. *Acta Crystallogr.* **1991**, *A47*, 405. (b) Nistor, L. C.; Tendeloo, G. V.; Amelinckx, S. *J. Solid State Chem.* **1994**, *109*, 152. (c) Tamada, O.; Yamamoto, N,; Mori, T.; Endo, T. *J. Solid State Chem.* **1996**, *126*, 1.
(29) Giacovazzo C. in *Fundamental Crystallography*; Giacovazzo C., Ed.; Oxford University Press: New York, 1992; Chapter 1, p 76.

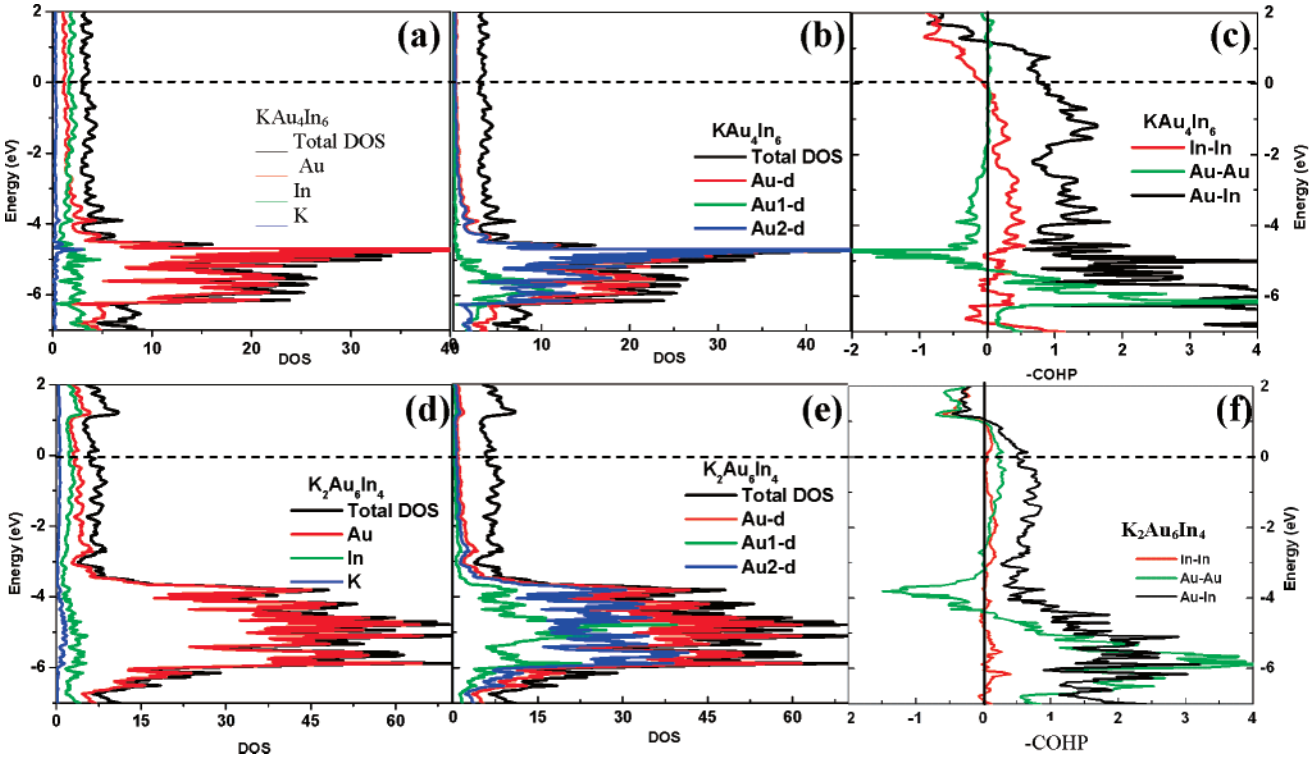

Figure 3. TB−LMTO−ASA electronic structure results for **I** (KAu_4In_6, top) and **III** ($K_{1.76}Au_6In_4$, bottom). (a, d) total DOS (black) and partial DOS curves for gold (red), indium (green), and potassium (blue). (b, e) total DOS (black) and partial DOS curves for the d orbitals of all gold (red), Au1 (green), and Au2 (blue). (c, f) Total −COHP data for three interactions in each structure: Au−In (black), In−In (red), and Au−Au (green). (The last two are minor in frequency.) The dotted lines denote the Fermi levels for the observed compositions of **I** and **III**.

the *ab* plane than along the *c* axis, consistent with the 6-9-6 ring arrangement, Figure 2a.

Electronic Structure and Chemical Bonding. The densities-of-states (DOS) for **I** (KAu_4In_6) and the idealized **III** ($K_2Au_6In_4$), Figure 3a and d, show broad bands with low total densities around E_F. Both Fermi levels intersect finite DOS, indicating metallic characteristics, and both **I** and **V** have been found to be Pauli-paramagnetic. The large peaks around −5 eV in both structures mainly originate from the Au d orbitals, Figure 3a and d. Substantially different contributions by Au d orbitals are shown in these two compounds, as well as by different Au sites in each structure. For **I**, Figure 3b, Au2 (3*k* site in the six-member ring) shows greater bonding than does Au1 (1*c* site in the nine-member ring). On the other hand, the much broader bands for Au in **III**, up to −3.5 eV, indicate stronger Au−Au interactions. Considering the different numbers of Au1 (8*h*) and Au2 (16*l*) in **III**, the total DOS contribution from each Au is similar, Figure 2e, but Au2 shows a broader band and more contributions at higher energies, up to about −3.5 eV, and Au1, narrower and at lower energies around −5.0 eV. The existence of Au2−Au2 bonds may be responsible for the broader band for Au2, which also holds true for the Au2 in **I**. In both cases, calculations that excluded scalar relativistic effects narrowed and moved these bands to just below −6 eV, as expected.

To compare the interactions between atoms, crystal orbital Hamilton population analyses (−COHP) were evaluated, as shown in Figure 3c and f for **I** and **III**, respectively. In **I**, strong bonding character is found for Au−In bonds in the 21-vertex polyhedra, and both Au−Au and In−In bonding are optimized at E_F. A greater number of electrons would populate In−In antibonding states and might lead to structural instability. Note that the number of Au−In bonds in the unit cell is more than 10 times that of In−In bonds, one reason for the relatively large −COHP values for the former. In **III**, both Au−In and Au−Au remain bonding at E_F whereas the In−In bond is substantially optimized. The absence of antibonding interactions for any of these up to 1 eV above the Fermi level indicates that it may be possible to form electron-richer isotypes (but this always depends on the stability of alternate phases as well). The integrated crystal overlap Hamilton populations (−ICOHP) were also determined. Those for Au−In in both compounds are almost same, about 1.2 eV/bond, which are comparable to those for Au−In in both KAu_4In_2[6] and Na_3AuIn_2.[2] As mentioned earlier, the polyhedral interbridging bonds Au2−Au2 (3.088 Å) and In1−In1 (3.335 Å) in **I** (Figure 1a) are quite long, but their −ICOHP values are not negligible, 0.69 and 0.34 eV/bond, respectively. The former is even larger than for the longer Au2−Au2 in **III** (0.37 eV/bond at 3.106 Å). Compared with the interbridging bond In1−In1, In1−In2 within the polyhedron in **I** has a similar length, 3.332 Å, but a larger −ICOHP, 0.47 eV/bond. These bonding characteristics, weaker between and stronger within polyhedra, are consistent with the overall drive for the formation of as many close neighbors as possible around each cation. The −ICOHP values for all K−In and K−Au are quite small in both structures, less than 0.1 eV/bond, and close to those in

KAu_4In_2,[6] indicating relatively weak cation−anion bonding contributions.

Conclusions

Following the discovery of KAu_4In_2 with a 1D tunnel structure, the formation of still other alkali-metal−Au−In analogues has suggested that derivatization of triel cluster phases by third elements may be a promising route to new compounds and structures. Six compounds exist in three different structure types with different three-dimensional Au−In frameworks filled with cations. However, the cations are differently trapped inside the tunnels in all because of apparently small free radii in the tunnels. It is interesting to note that **III**, **IV**, and KAu_4In_2[6] all have similar K/(Au + In) proportions but markedly different structures that follow changes in the Au/In proportions. The 1D tunnels get larger with increases in indium proportions, so it might be possible to gain more open tunnels with larger anions by substituting Tl for Au or In.

Acknowledgment. We are indebted to Dr. Ingo Pantenburg and Prof. Gerd Meyer in the University of Cologne for the collection of low-temperature single-crystal X-ray diffraction data for $K_{0.73}Au_2In_2$ (**IV**) and to Dr. Sergey Bud'ko for the magnetization data for **I** and **IV**. This research was supported by the Office of the Basic Energy Sciences, Materials Sciences Division, U.S. Department of Energy (DOE) and performed in the Ames Laboratory, which is operated for DOE by Iowa State University under Contract No. DE-AC02-07Ch11358.

Supporting Information Available: Refinement parameters for KAu_4In_6 (**I**), $RbAu_4In_6$ (**II**), $K_{1.76(6)}Au_6In_4$ (**III**), $K_{0.73(5)}Au_2In_2$ (**IV**), $Rb_{0.66(2)}Au_2In_2$ (**V**), and $Cs_{0.66(1)}Au_2In_2$ (**VI**) in cif format, figures of electronic density maps around the cations in **III**, **IV**, **V**, and **VI**, and representations of the K neighbors in **I**, **III** and **IV**. This material is available free of charge via the Internet at http://pubs.acs.org.

IC700519C